Development of Optical Filters Based on Photorefractive Materials

Paul R. Schuster, Joseph A. Miragliotta, Michael E. Thomas, and David M. Rust

Photorefractive optical filters meet many of the very stringent requirements of modern electro-optic systems. They provide a narrow passband and good throughput. However, difficulties arise when designing a filter to operate at wavelengths where the photorefractive material has low sensitivity. We have demonstrated initial success in overcoming the frequency dependence. This task was accomplished by using an optical configuration of high sensitivity in terms of wavelength, incident angle, and polarization to generate prespecified grating spacings. The grating spacings were designed to satisfy Bragg conditions for efficient operation of the filter (diffraction efficiency) even when using lower sensitivity wavelengths and alternative geometries of interest.

INTRODUCTION

High-speed electro-optic systems with narrowband spectral resolution and tunability are of interest for optical filtering within a variety of applications. Global climate change and airborne pollution have created a need for spectral imaging devices with sufficient sensitivity and wavelength resolution to measure minute concentrations of atomic and molecular constituents of the air. It will be important to map narrow spectral lines quickly and efficiently over large fields of view. For example, for determinations of the spatial variation of the energy losses and inputs at various levels of the atmosphere, hydroxide, nitrogen oxide, and carbon dioxide emission line profiles need to be studied with high temporal and spatial resolution. Spectral remote sensing can also be applied in differential absorption lidar (DIAL, see boxed insert) to provide critical information about conditions within the atmosphere that may adversely affect the propagation of various electromagnetic waves used for communications, radar, environmental and ecological monitoring, etc.

Improved spectral imaging is needed in astronomy, too. For example, maps of solar surface magnetic fields can be constructed from measurements of the polarization in spectral lines that are sensitive to the Zeeman effect.[1] These maps can be used to develop techniques to forecast solar activity and its effects on communications and satellite orbits. Also, as discussed by Kunches et al.,[2] manned exploration of space beyond Earth's magnetosphere will require substantial improvements in the reliability of solar activity forecasts. Without good forecasts, the freedom of astronauts to carry out extravehicular activities will be limited because of the threat of lethal or disabling protons from flares. Since all solar activity arises from the action of solar magnetic fields, we are interested in making as precise measurements of these fields as possible.

Optical communications offer another important application for tunable optical filters. Fibers can carry much more information if many wavelengths can be used simultaneously, as in wavelength-division multiplexing. The resolution of the demultiplexor, i.e., its ability to uniquely define individual data channels, determines the capacity of the system. Demultiplexors must be very fast and require little power to operate.

Differential absorption lidar (DIAL) is a common remote sensing technique that uses two signal frequencies from a transmitter device. One signal is tuned to line center of an absorption line, while the other frequency is tuned to a nearby spectral location with little or no absorption. Such a system measures the average transmittance over a range cell at both on- and off-line frequencies. From the average, the line center absorption coefficient at that location in space can be determined. Subsequently, species concentration or temperature can be inferred. This technique is typically accomplished through the use of a stable, tunable, narrowband laser of high spectral purity. However, the use of simpler broadband lasers such as optical parametric oscillators is possible. There is growing interest in DIAL because the technology can be applied at eye-safe infrared frequencies.

The use of broadband (approximately 0.03- to 0.04-μm bandwidth) lasers in gas-phase remote sensing is not a new concept.[3,4] The novelty of the proposed APL approach is the use of a broadband laser with a photorefractive "broadband" filter (approximately 0.01-μm bandwidth) in the receiver of a DIAL system. The concept is illustrated in the figure for the transmittance of an absorption line located at 10 μm. The three transmittance curves represent different path lengths.

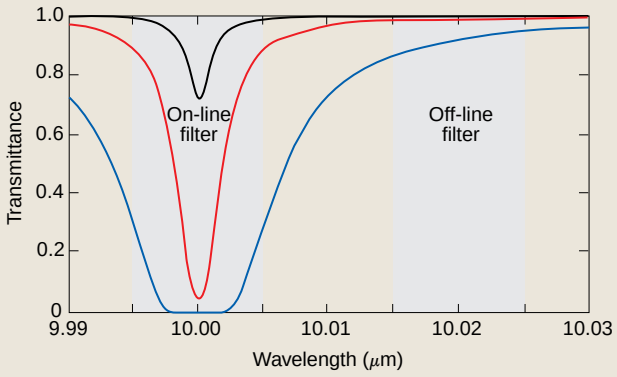

Broadband DIAL concept of a single laser pulse with a bandwidth of 0.04 μm and a receiver with two 0.01-μm bandwidth filters, one for on-line and the other for off-line. The three transmittance curves represent different path lengths.

The shaded areas define the spectral ranges of the off-line and on-line filters. This approach is less complex and therefore less expensive than the cost of narrowband DIAL systems and offers some performance advantages as well. Broadband transmittance is virtually insensitive to line shift errors and less sensitive to halfwidth errors relative to common narrowband DIAL. A filter in the receiver is needed to separate on-line and off-line spectral information. The filter must be tuned to be nearly centered on the absorption feature, with a resolving power of approximately 6000 ($\lambda/\Delta\lambda$). The tunability of the filter will allow multiple absorption lines to be probed for extending spatial range or the measurement of other atmospheric quantities. This is an ideal application of a photorefractive tunable filter.

Spectral imaging plays a critical role in many other remote sensing applications. When imaging is performed using a large-aperture, tunable filter coupled with a digital charge-coupled-device camera, e.g., a Kodak Megaplus with 1538×1024 pixels and 20-frames/s readout rate, then image spectral content can be measured with high speed and precision. We propose to use a photorefractive $LiNbO_3$ filter as a prefilter for a solid Fabry-Perot étalon (coincidentally also made of $LiNbO_3$ because of its tunability with high voltage). Solid étalons have a great advantage over the more familiar air-spaced ones. They are rugged enough for field applications, and they are insensitive to air pressure and temperature.

Étalons made of $LiNbO_3$ have two series of passbands distributed across a broad spectral region.[5] One set of bands can be scanned in wavelength by application of voltage while the other remains relatively fixed. We intend to use the tunability and the reference passband qualities of a hybrid étalon/photorefractive filter to make sensitive measurements of atmospheric absorption and emission lines.

In solar research, the sensitivity of Zeeman effect measurements has been limited by relatively wide passbands and slow-tuning. One version of the filter combination we are proposing will have a passband of only 50 mÅ and a tuning rate of 20 frames/s (with a change in wavelength for each frame). Together, a 4-Å photorefractive blocking filter and a 0.05-Å étalon will be able to isolate a small part of the profile of a magnetically sensitive iron line in the solar spectrum. Data on the solar magnetic fields can then be gathered by scanning through the line.

Other examples of applications that should benefit from improved spectral filtering include frequency-stabilized laser systems and laboratory spectroscopy.

Advanced Optical Filters

To achieve the performance required, new sensing systems with greatly improved optical filters, i.e., filters that provide sub-angstrom spectral resolution, rapid wavelength tuning, low wavefront distortion (for imaging), and high throughput, will be needed. The challenge in remote sensing is to provide rugged, easily used, relatively inexpensive devices that can project an image of contaminant concentrations on a screen and record measurements for long-term research. The challenge in optical communications is to integrate extremely inexpensive and rapidly tunable devices into existing systems.

A number of different types of filters exist that meet many of the required specifications. These filters include interference filters produced from multilayer structures and Fabry-Perot étalon filters such as the Lyot filter, which serve as fixed interferometers. The Lyot filter is currently the preferred approach for applications requiring very high spectral resolution.[5] However, for optical filtering applications, Rakuljic

and Leyva[6] and Müller et al.[7] recently demonstrated the use of holographically generated, high-spatial-frequency diffraction gratings within photorefractive materials.

The photorefractive filter has several advantages including cost, size, versatility, speed, and weight. A disadvantage is the strong frequency-dependent nature of the photorefractive sensitivity for the most commonly used materials. This problem is evident in the time required to create the filter (write the grating) and the diffraction efficiency (performance) during operation.

The research efforts discussed in this article focused on overcoming the deficiencies by using an optical configuration of high sensitivity in terms of wavelength, incident angle, and polarization in order to write holographic gratings with prespecified spacings. The grating spacings were designed to satisfy Bragg conditions for efficient operation of the filter, even when using lower sensitivity wavelengths and alternative geometries of interest.

THEORETICAL APPROACH

The photorefractive material used in this research was the ferroelectric oxide lithium niobate ($LiNbO_3$) in bulk, single-crystal form. The photorefractive properties of this material have been extensively studied and are very well documented.[8–10] Iron-doped $LiNbO_3$ has relatively high photorefractive sensitivity in the visible portion of the spectrum, especially at the higher frequencies, as a result of its large electro-optic coefficient. It is also convenient to work with and easy to align for photorefractive applications because of its symmetry and the orientation of its most effective crystallographic direction. The largest electro-optic coefficient is along the polarization axis (*c* axis).

Within photorefractive materials, a spatially inhomogeneous charge density can be induced when they are illuminated with a coherent light source. Generally, the charge density originates from either impurities or defects within the crystal or from dopants deliberately introduced into the material. When two mutually coherent light beams interact within the photorefractive material, a spatial interference pattern is created in the bulk of the media, which induces the charge density to migrate from a steady-state equilibrium distribution into a new spatial profile that mimics the optical pattern (Fig. 1). The charge migration induces a static electric field inside the crystal, which generates a first-order change (Pockels effect) in the material's refractive index (Δn):

$$\Delta n = \frac{1}{2} n^3 r_{ij} E_{sc},$$

where r_{ij} is the Pockels coefficient (electro-optic tensor component) and E_{sc} is the space–charge field. The index profile has the same spatial distribution as that of the charge density in the crystal. Under the proper illumination conditions, periodic variations can be created in the refractive index, which act as a highly selective wavelength- and orientation-specific diffraction grating, in a manner similar to a volume hologram stored within thick, high-resolution holographic film. (For a comprehensive discussion on Bragg diffraction and optical holography, see Ref. 11.)

The spatial periodicity of the index grating can be fixed by thermal treatment, creating a long-term (semipermanent) diffraction pattern within the photorefractive material. In addition, wavelength tunability may be accomplished by changing the average refractive index or the grating period via an externally applied voltage or temperature source.[12] This method eliminates the need for mechanical systems that are commonly used in the tuning of more conventional grating elements.

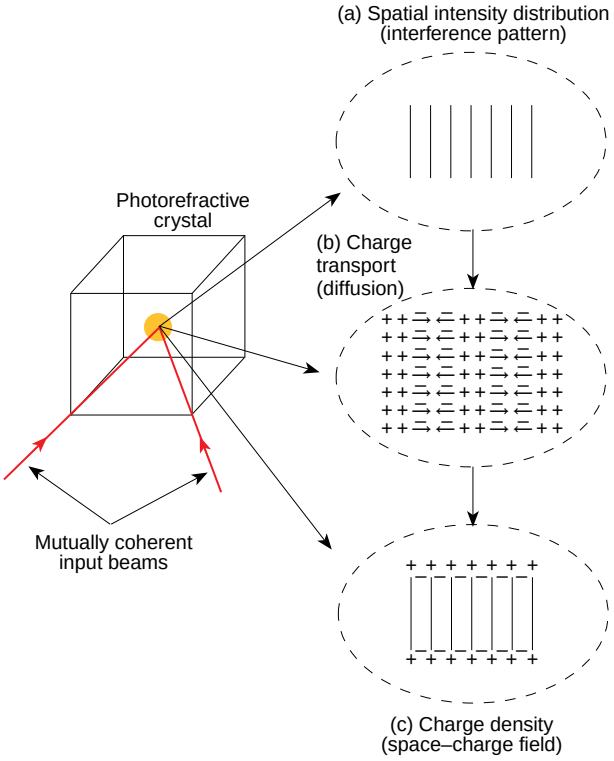

Figure 1. Interaction of two mutally coherent beams within a photorefractive crystal. (a) A unique spatial intensity distribution is formed within the material resulting from the interference of the two waves. (b) Charges diffuse from regions of high intensity and are trapped in regions of low intensity. (c) The separation of charges leads to the creation of a space–charge field.

To take full advantage of the photorefractive sensitivity within these materials, certain parameters must be evaluated. These parameters include the preferred wavelength (material's sensitivity) for writing, angular position and polarization of the incident waves, *c*-axis orientation of the photorefractive crystal, and the ratio of incident beam intensities. As stated earlier, since the sensitivity of iron-doped $LiNbO_3$ is wavelength or frequency dependent, the writing wavelength may be different than the filter's actual operating wavelength. The filter's performance is then based on its ability to match Bragg conditions for diffraction at the desired wavelength and optical configuration. Therefore, the wavelength, angular position, and wavefront characteristics of the incident writing beams are dictated by the filter's desired operating wavelength, the angular position and wavefront characteristics, the refractive index of the material at both the writing and reconstructing wavelengths, and the desired optical configuration (transmission or reflection) for operation of the filter.

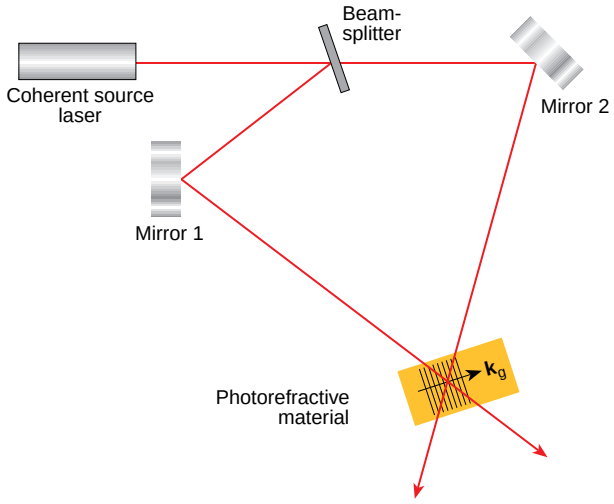

Figure 2. Experimental configuration for transmission holography used to write holographic diffraction gratings within the $LiNbO_3$ sample. ($\mathbf{k}_g$ is the grating vector.)

EXPERIMENTAL APPROACH

Initial gratings were written in a $5 \times 5 \times 5$ mm cube of iron-doped $LiNbO_3$ using an argon laser (coherence length about 2 cm) at both 488.0 nm and 514.5 nm. This crystal was doped with 0.05% iron for increased sensitivity in the visible portion of the electromagnetic spectrum. Setting up the optical system, writing the gratings, and characterizing their performance at the original wavelength were successful for both the transmission mode (Fig. 2) and also the higher resolution reflection mode (Fig. 3). Writing the hologram at one argon line and reading it out at another resulted in only a minor reduction in the signal-to-noise ratio. However, as the variation between the writing and reconstructing wavelengths (and coherent sources) is increased, a number of other issues have to be considered.

As stated earlier, these materials can be used broadband, but their sensitivity (absorption) is frequency dependent. Therefore, gratings were written at wavelengths of high sensitivity for operation at regions of lower sensitivity. Initially, a symmetrical transmission approach (symmetrical around the normal to the crystal's *a* face) was utilized at a relatively small angular separation ($2\theta \leq 50°$) between the object and the reference wave (low-resolution grating) (Fig. 4). This approach was taken to minimize the refractive index effects of the material, which change both the position and angular relationship of the incident waves, thereby affecting the grating spacing within the material. At a larger angular separation between the writing waves, a more selective filter is formed as a result of a smaller grating spacing with more grating planes per unit volume of material.

Initially, gratings were written (filter formation) at the argon line of 514.5 nm, and the performance of the filter was evaluated at a region of lower sensitivity[13] using a helium–neon laser at 632.8 nm. In general, for the reflection mode of operation, the situation becomes even more complex and stringent regarding acceptable wavelengths and range of incident angles for writing the gratings. The frequency-dependent refractive index of the material begins to have a more significant effect, especially when the gratings are formed in transmission through the *a* face of the crystal and utilized in the reflection mode through the *c* face (Fig. 5).

To differentiate the diffracted wave of interest from all the other propagating waves and the various reflections, a two-dimensional object (35-mm slide) was placed in the path of one of the incident writing beams, thereby creating a true object wave. The object wave

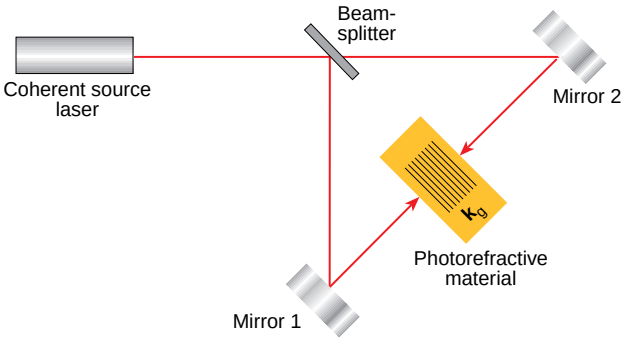

Figure 3. Experimental configuration for reflection holography used to write higher resolution holographic diffraction gratings within the $LiNbO_3$ sample. ($\mathbf{k}_g$ is the grating vector.)

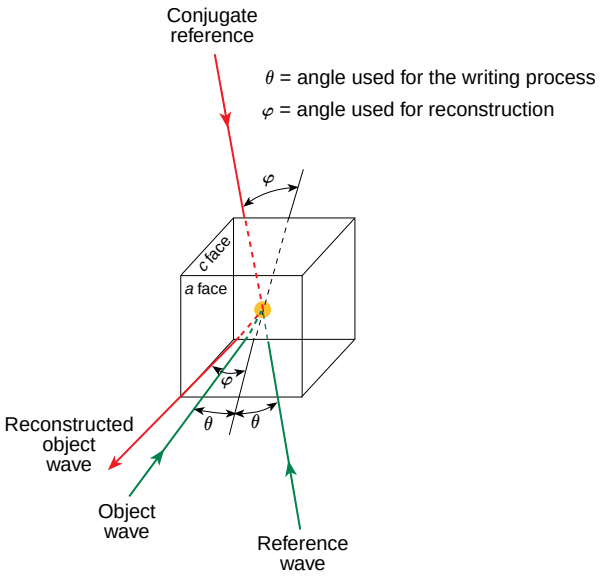

Figure 4. Symmetrical transmission approach used to write gratings at a particular wavelength and geometry, but designed for operation at a different wavelength and corresponding incident angle.

was then focused through the crystal for interference with the collimated reference wave. Therefore, on reconstruction of the hologram, it was possible to re-create the object wave and project a real image onto a screen of the two-dimensional object. When a wavelength similar to that used in writing the hologram (within 50 nm) was used on reconstruction, the diffracted wave was readily identifiable. Reconstruction with a collimated reference wave at a dramatically different wavelength than that used in writing greatly diminished the reconstructed spatial frequencies that described the original object. This effect was due to the optical configuration used in the formation of the holographic filter.

The object wave propagated with a spherical wavefront, but the reference wave was collimated (planar wavefront); therefore, the waves' interference within the crystal produced an angular tilt to the grating

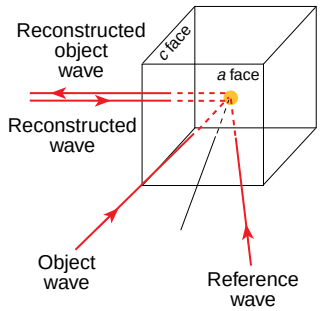

Figure 5. Symmetrical transmission approach used to write gratings at one wavelength for use in reflection at a different wavelength.

planes formed.[14] These events resulted in a situation during reconstruction where the desired plane wave reference, at a different wavelength than that used for writing, was unable to simultaneously match the Bragg conditions for all spatial frequencies contained within the original object wave.[15] The consequence of such a condition was that during reconstruction, only a slice of the original object wave was regenerated, producing only a section of the original image.

Initially, filters were generated at 514.5 nm using ordinary polarization and an angle of 25° to the surface normal in the symmetrical transmission holographic configuration (Fig. 4). At the 632.8-nm wavelength used for reconstruction, the Bragg angle required was about 31° for evaluation of the filter's performance. The optical system used for the performance characterization of the photorefractive samples consisted of a neodymium-doped yttrium aluminum garnet (Nd:YAG) laser (10-Hz repetition rate, 10-ns pulse width, 1064-nm or 532-nm output), tunable dye laser, and high-pressure hydrogen Raman cell (Fig. 6). The output of the nanosecond dye laser, which is pumped by the 532-nm output of the Nd:YAG laser, is tunable through the 550- to 900-nm wavelength range. This spectral output can be used as either a visible- to near-infrared light source in characterization measurements or as the optical pump for generating longer wavelength infrared via coherent Raman scattering in the hydrogen gas ($\lambda = 0.8$–$2.0\ \mu$m). In addition to the wide range of tunability, the high spectral resolution of the optical system ($\Delta\lambda \approx 0.01$ Å) surpassed the grating resolution in the photorefractive iron-doped $LiNbO_3$ samples.

EXPERIMENTAL RESULTS

The filter demonstrated an approximate 5-nm full width at half maximum bandwidth at less than 5% diffraction efficiency when using a nonoptimized, low-resolution optical setup (Fig. 7). After the successful demonstration of the feasibility of this approach, the next step was to write higher resolution gratings in the $LiNbO_3$ crystal. Because of the dimensions of the photorefractive crystal with a 5×5 mm entrance face, a limitation exists on the angular separation between the object and reference waves. The angular separation also depends on the diameter of the incident beams. The symmetrical transmission approach was used for generating these higher resolution filters.

Various writing conditions were evaluated. It was determined that formation of a grating for subnanometer resolution could be successfully accomplished at the writing wavelength of 514.5 nm with an angle of incidence for both object and reference waves of 45° to the normal to the *a* face, using ordinary polarization. Optical characterization (reconstruction) took place

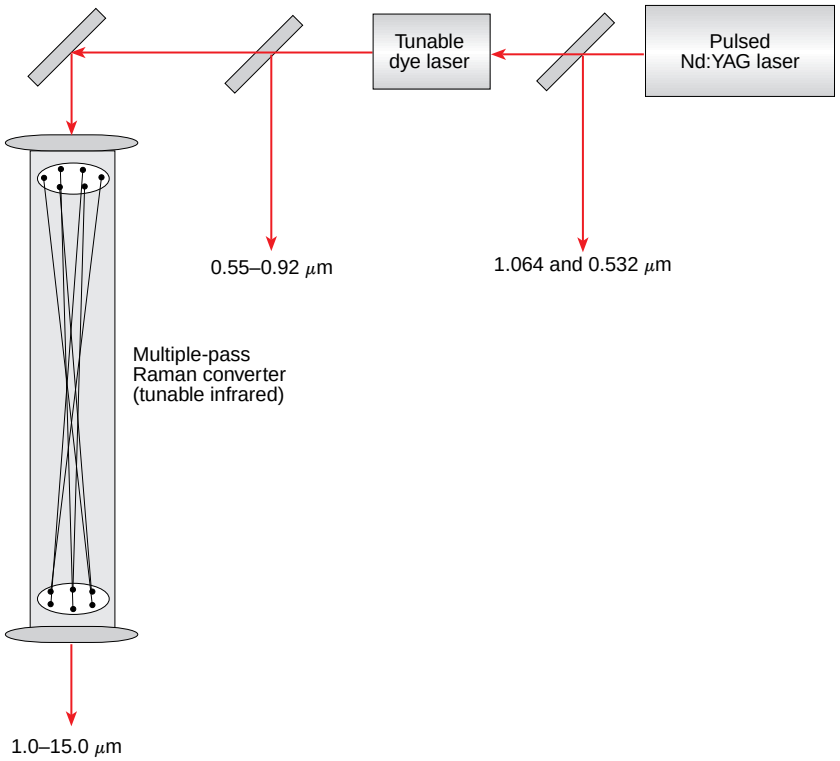

Figure 6. The optical system for characterization and performance assessment of the photorefractive filter. Laser source provides tunable radiation from 0.55 to ≈10 μm. Nd:YAG provides discrete laser lines at 1.064 and 0.532 μm. The bandwidth of the laser radiation over this range of wavelengths is sub-angstrom.

at a variety of incident angles and wavelengths; however, a representative data plot is presented in Fig. 8 for the center peak wavelength of 654.8 nm. The incident angle required to match Bragg conditions for operation at this wavelength was approximately 64.5°.

The results from this analysis indicated the filter's performance to be better than 0.6-nm full width at half maximum bandwidth wavelength selectivity, nearly an order of magnitude improvement over the previous results (Fig. 7). In the data shown in Fig. 8, note the higher background intensity (DC bias) as compared with the data in Fig. 7. This effect was due to the increased internal scattering in the $LiNbO_3$ sample. The photorefractive behavior was directly related to the fluence or power density and spatial intensity profile of the incident beams. Therefore, when the filter's performance is evaluated, the reconstructing wave (Gaussian profile-TEM_{00}) will adversely affect the existing hologram. The signal-to-noise ratio decreased through the duration of the reconstruction process (Fig. 9). This decrease resulted from both an increase in scatter and a reduction in the depth of the modulation within the hologram.

DISCUSSION

Techniques that should improve both the signal-to-noise ratio and the spectral resolution include erasing the pre-existing holograms before writing new ones, fixing the desired grating, and optimizing the incident angle for reconstruction. Because the dark conductivity is low (limited residual charge migration) in $LiNbO_3$,[16] holograms formed in this material are very persistent and can last from hours to days, even without fixing. However, when it was desirable to change the optical system for writing higher resolution gratings, these persistent holograms produced tremendous noise and distortion. Therefore, it was

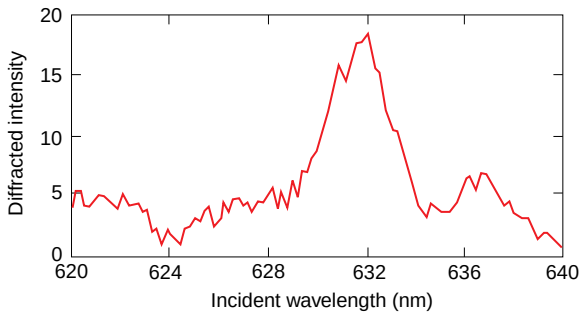

Figure 7. Diffracted intensity (in arbitrary units) versus wavelength for a photorefractive optical filter during reconstruction at 632.8 nm. The filter was created using a 514.5-nm coherent source.

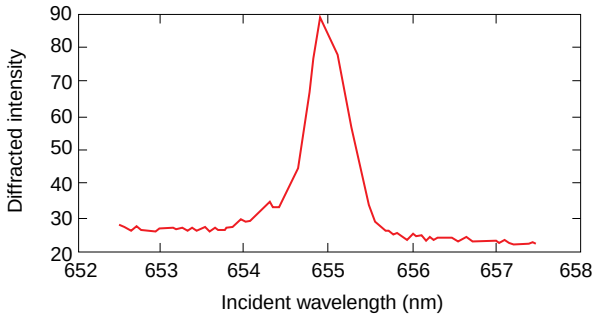

Figure 8. Filter performance evaluation (diffracted intensity [in arbitrary units] versus wavelength) demonstrates an operating bandwidth of ≈0.5 nm for 654.8-nm center wavelength at an incident angle of 64.5°. The filter was created using 514.5 nm at 45° in transmission.

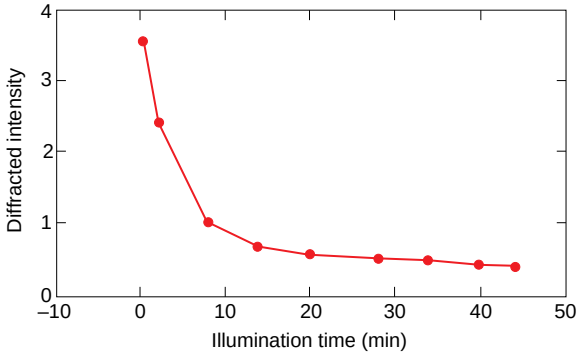

Figure 9. Diffracted intensity (in arbitrary units) versus sample illumination time. This plot illustrates the destructive nature of the "reconstruction" process (which occurs on a time scale of ≈4–5 min) when the incident laser intensity used was ≈10 mW/mm^2.

necessary to develop an approach for erasing the preexisting gratings before writing new ones. From the literature[7] and from experimental investigation, it was determined that for complete erasure, the crystal should be heated to about 250°C for about 1 h. The crystals proved to be very durable and did not require a particularly slow temperature ramp either up or down.

A technique for fixing the grating was also established. Again, from the literature[17] and experimental investigation, it was determined that an acceptable fixing approach involved the following steps: (1) write the desired hologram, (2) heat the crystal in the dark up to approximately 125°C, (3) hold the crystal at 125°C for about 5 min, (4) bring the crystal back down to room temperature, and (5) expose the crystal to the reconstructing wave with a uniform spatial intensity distribution (TEM_{00}) for approximately 10 min before making any measurements.

The success of this technique is based on both the ionic and electronic conductivity for iron-doped $LiNbO_3$ at various temperatures. At room temperature, electrons are mobile under the influence of the incident coherent radiation; the optical interference produces a space–charge field that results in a refractive index change (hologram) within the material. Once the hologram is formed, the material is no longer in a neutral state. Therefore, at elevated temperatures where the ionic mobility dramatically increases, the ions redistribute in an attempt to neutralize the existing space–charge field. When the crystal is returned to room temperature, the ions no longer have the thermal activation energy required for mobility; therefore, the existing ionic distribution is fixed. This ionic distribution now mimics the original spatial intensity distribution created by the interference of the object and reference waves.

The next step is to uniformly redistribute the electrons, which are mobile at room temperature, by illuminating the crystal with a reconstructing wave of uniform spatial intensity. Although this method has proved successful, a recent study indicates that a slightly different fixing approach will yield a dramatic enhancement to the filter's performance. Müller et al.[7] demonstrated an increase in diffraction efficiency of more than an order of magnitude by not only simultaneous writing and fixing of the grating, but also by short-circuiting the crystal faces during temperature elevation (to minimize photovoltaic effects). The use of these techniques should generate an increased depth of modulation within the hologram, improving the diffraction efficiency and providing a higher signal-to-noise ratio during operation.

CONCLUSION

Photorefractive optical filters can meet the specifications of a variety of electro-optic systems. Operating characteristics such as sub-angstrom spectral resolution, high signal-to-noise ratio, tunability, and high speed make these filters extremely attractive for signal processing–intensive applications including remote sensing, monochromatic imaging, and optical communications. The frequency-dependent nature of these filters has limited their use to within a very narrow portion of the electromagnetic spectrum. However, research efforts, supported by Independent Research and Development funds, have demonstrated preliminary success in overcoming this problem by creating prespecified diffraction gratings with grating spacing designed to match Bragg conditions for alternative wavelengths and geometries of interest. The relatively low-cost, lightweight, and compact nature of these photorefractive filters provides an additional incentive for their use.

REFERENCES

[1] Rust, D. M., and O'Bryne, J. W., "Vector Magnetography," in *Solar Polarimetry*, National Solar Observatory, Sunspot, NM (1991).
[2] Kunches, J. M., Heckman, G. R., Hildner, E., and Suess, S. T., "Solar Radiation Forecasting and Research to Support the Space Exploration Initiative," in *Solar Radiation Forecasting*, NOAA Space Environment Lab, Boulder, CO (1991).
[3] Theopold, F. A., Weitkamp, C., and Michaelis, W., "BELINDA: Broadband Emission Lidar with Narrowband Determination of Absorption, A New Concept for Measuring Water Vapor and Temperature Profiles," in *Sixteenth International Laser Radar Conference*, NASA Conference Publication 3158, Part 2, pp. 671–674 (1992).
[4] Edner, H., Svanberg, S., Unéus, L., and Wendt, W., "Gas-Correlation Lidar," *Opt. Lett.* **9**, 493–495 (1984).
[5] Rust, D. M., "Étalon Filters," *Opt. Eng.* **33**(10), 3342–3348 (1994).
[6] Rakuljic, G. A., and Leyva, V., "Volume Holographic Narrow-Band Optical Filter," *Opt. Lett.* **18**(6), 459–461 (1993).
[7] Müller, R., Santos, M. T., Arizmendi, L., and Cabrera, J. M., "A Narrow-Band Interference Filter with Photorefractive $LiNbO_3$," *J. Phys. D: Appl. Phys.* **27**, 241–246 (1994).
[8] Arizmendi, L., and Agulló-López, F., "$LiNbO_3$: A Paradigm for Photorefractive Materials," in *MRS Bull.* **XIX**(3), 32–38 (Mar 1994).
[9] Staebler, D. L., and Phillips, W., "Fe-Doped $LiNbO_3$ for Read-Write Applications," *Appl. Opt.* **13**(4), 788–794 (1974).
[10] Amodei, J. J., and Staebler, D. L., "Holographic Recording in Lithium Niobate," *RCA Rev.* **33**, 71–93 (1972).

[11] Collier, R. J., Burckhardt, C. B., and Lin, L. H., *Optical Holography*, Academic Press, Orlando, FL (1971).
[12] Müller, R., Alvarez-Bravo, J. V., Arizmendi, L., and Cabrera, J. M., "Tuning of Photorefractive Interference Filters in $LiNbO_3$," *J. Phys. D: Appl. Phys.* **27**, 1628–1632 (1994).
[13] Phillips, W., Amodei, J. J., and Staebler, D. L., "Optical and Holographic Storage Properties of Transition Metal Doped Lithium Niobate," *RCA Rev.* **33**, 94–109 (1972).
[14] Latta, M. R., and Pole, R. V., "Design Techniques for Forming 488-nm Holographic Lenses with Reconstruction at 633 nm," *Appl. Opt.* **18**(14), 2418–2421 (1979).
[15] Kulich, H. C., "A New Approach to Read Volume Holograms at Different Wavelengths," *Opt. Commun.* **64**(5), 407–411 (1987).
[16] Gunter, P., and Huignard, J.-P., "Optical Processing Using Wave Mixing in Photorefractive Crystals," Chap. 6, in *Photorefractive Materials and Their Applications II*, Springer-Verlag, Berlin, p. 221 (1988).
[17] Arizmendi, L., Townsend, P. D., Carrascosa, M., Baquedano, J., and Cabrera, J. M., "Photorefractive Fixing and Related Thermal Effects in $LiNbO_3$," *J. Phys.: Condens. Matter* **3**, 5399–5406 (1991).

ACKNOWLEDGMENT: This research was supported by Independent Research and Development funding in the Photonics and Electro-Optics Thrust Area under the direction of Harry K. Charles, Jr.

THE AUTHORS

PAUL R. SCHUSTER is a Materials Scientist and Senior Staff member in the Advanced Signal and Information Processing Group of APL's Milton S. Eisenhower Research Center. He has B.E.S, M.S.E., and Ph.D. degrees in materials science and engineering from The Johns Hopkins University. While in school, Dr. Schuster served as an Engineering Officer in the Public Health Service working in the areas of biomedical engineering and medical devices. He then joined APL's Research Center in 1988. He received the Outstanding Scholar Award from the ARCS Foundation (1985–86) and the Peterson Award for his research from the Society for Experimental Mechanics (1990). He has held a joint appointment in the Whiting School of Engineering since 1992. His research interests include optical properties of materials, materials fabrication, techniques for optical metrology, and sensory engineering. His e-mail address is Paul.Schuster@jhuapl.edu.

JOSEPH A. MIRAGLIOTTA is a Physicist and Senior Staff member in the Sensor Science Group of APL's Milton S. Eisenhower Research Center. He received a B.S. in physics from Manhattan College in New York in 1982 and M.S. and Ph.D. degrees in physics from Rensselaer Polytechnic Institute in 1985 and 1987, respectively. Before joining the Laboratory, he was involved with the development of a nonlinear optical program at Exxon Research and Engineering for surface studies pertaining to lubrication and corrosion inhibition at liquid/solid interfaces. Since joining the Research Center in 1990, he has developed a nonlinear optical program devoted to the spectroscopic analysis of surfaces, compound semiconductors, and thin-film waveguide devices. Dr. Miragliotta has conducted research in surface-enhanced Raman scattering, photoluminescence of semiconductors, and optical scattering in biomedical systems. He is a member of the American Physical Society, the Optical Society of America, the Materials Research Society, the IEEE, and SPIE. His e-mail address is Joseph.Miragliotta@jhuapl.edu.

MICHAEL E. THOMAS obtained a B.E.E. degree from the University of Dayton in 1973, and M.S. and Ph.D. degrees from Ohio State University in 1976 and 1979, respectively. Since joining APL in 1979, he has worked on electromagnetic propagation and optical properties of materials. In 1982, he was a postdoctoral fellow in the Department of Physics at the Naval Postgraduate School. In 1988, Dr. Thomas became a faculty member of the Part-Time Programs in Engineering and Applied Science at The Johns Hopkins University G.W.C. Whiting School of Engineering, teaching courses on optical propagation and lasers. His current research interests include experimental and theoretical modeling of atmospheric propagation in the infrared, differential absorption lidar, optical and infrared window materials, and the infrared properties of high-pressure gases. He has published over 65 articles in books and journals. His e-mail address is Michael.Thomas@jhuapl.edu.

DAVID M. RUST received his Sc.B. degree in physics from Brown University and his Ph.D. in astro-geophysics from the University of Colorado. A member of the Principal Professional Staff at APL and Solar Physics Section Supervisor, Dr. Rust has initiated programs to analyze solar X-ray emissions; build new solar telescopes, optical filters, and detectors; and map solar surface magnetic fields. He also established the APL Solar Observatory. He has published over 80 refereed papers on polarimetry, filters, and other instruments, as well as the effects of solar magnetic fields and solar flares on manned activity in space. His current interests include development of fully tunable, ultranarrow bandpass optical filters for remote sensing applications. His e-mail address is David.Rust@jhuapl.edu.